A semi-empirical model for hermetic rolling piston compressors

Luca Molinaroli *, Cesare Maria Joppolo, Stefano De Antonellis

Dipartimento di Energia, Politecnico di Milano, Via Lambruschini 4, 20156 Milano, Italy

Rolling piston compressors are widely used in many low capacity refrigeration and air con-ditioning systems as they have advantages over reciprocating compressors. Current models of this compressor technology available in the scientific literature are mainly determinis-tic models, i.e. models that need a minute description of compressor geometry, whereas for other compressor technologies, such as reciprocating, scroll and screw ones, semi-empirical models are successfully used in simulating compressor operations. Therefore, this paper introduces a semi-empirical model of a rolling piston compressor and validates it by considering four different compressors, designed for different applications and working with different refrigerants, in order to achieve a good degree of generality for the model. Overall, 240 performance data were considered and an agreement within ±5% was found for more than the 96% of the calculated refrigerant mass flow rates and more than 97% of the calculated compressor electrical powers.

Keywords: Modelling, Rolling piston compressor, Semi-empirical model

Modèle semi-empirique pour les compresseurs hermétiques à piston roulant

Mots clés : Modélisation ; Compresseur à piston roulant ; Modèle semi-empirique

1. Introduction

Rolling piston compressors are low capacity compressors used in many refrigeration and air conditioning systems. With respect to similar low capacity compressors, namely reciprocating compressors, the rolling piston compressors exhibit a number of advantages such as a simpler design and operation at higher rotational speed, easier lubrication of moving parts due to their compactness, and higher resistance to possible refrigerant liquid droplets at the compressor suction. Overall, their low volume, weight and cost combined with high performance make the rolling piston compressors increasingly popular in low capacity air conditioning and refrigeration systems.

In this context, a mathematical model of rolling piston compressors may be a useful tool in their design or in analysing systems in which they are installed, whether from a general system operation or a control perspective. Indeed, although many studies in the open literature deserved attention to the simulation of rolling piston compressors, the mathematical models available are, with only one exception, deterministic or geometrical models, meaning that they require a detailed description

Article history:
Received 15 November 2016
Received in revised form 15 April 2017
Accepted 17 April 2017
Available online 21 April 2017

* *Corresponding author.* Dipartimento di Energia, Politecnico di Milano, Via Lambruschini 4, 20156 Milano, Italy. Fax: +39 02 23993913.
E-mail address: luca.molinaroli@polimi.it (L. Molinaroli).

Nomenclature

a	coefficient to be used in Eq. (34) [measurement units: see Table 4]
A	area [m^2]
a	coefficient to be use in Eq. (35) [measurement units: see Table 4]
e	error [dimensionless]
c_P	isobaric specific heat [$J \cdot kg^{-1} \cdot K^{-1}$]
f	rotational frequency [Hz]
h	enthalpy [$J \cdot kg^{-1}$]
$\dot{m}$	mass flow rate [$kg \cdot s^{-1}$]
NTU	number of transfer unit [dimensionless]
p	pressure [kPa]
$\dot{Q}$	heat transfer rate [W]
s	entropy [$J \cdot kg^{-1} \cdot K^{-1}$]
T	temperature [K]
UA	overall heat transfer coefficient [$W \cdot K^{-1}$]
V	swept volume [m^3]
$\dot{v}$	volumetric flow rate [$m^3 \cdot s^{-1}$]
$\dot{W}$	power [W]

Greek symbols

α	coefficient of proportionality in losses expression [dimensionless]
γ	ratio of isobaric to isochoric specific heat capacity [dimensionless]
ε	effectiveness [dimensionless]
ρ	density [$kg \cdot m^{-3}$]

Subscripts

1...5	refrigerant state
AMB	ambient
CALC	calculated
COMP	compressor
COND	condensing
CRIT	critical
DIS	discharge
EVAP	evaporating
IC	isentropic compressor
INT	internal
LEAK	leakage
LOSS	lost
MAN	manufacturer
RE–EXP	re-expansion
REF	reference
SUC	suction
THR	throat
TOT	total
W	wall

of the geometry of the compressor in order to compute the state of the refrigerant during its path inside the compressor.

Ooi and Wong (1997) developed and validated a deterministic model of a fixed speed rolling piston compressor. The validation was carried out considering three different compressors, working with R12, R22 and R134a respectively. The model was highly accurate at predicting the refrigerant mass flow rate since numerical data agreed with experimental data to within –1.4% to +0.6%. The prediction of the compressor electrical power was slightly less accurate since numerical data agreed with experimental values to within –10.5% to –2.4%.

Using the model previously developed and validated, Ooi (2005) carried out an optimization procedure with the aim of reducing the compressor mechanical losses given compressor operating conditions and swept volume. The optimization was carried out by varying specific geometrical parameters of the compressor such as cylinder radius, shaft radius, eccentricity radius, etc., and it was found that an increase of +14% in the overall mechanical efficiency can be achieved.

Ooi and Lee (2008) used the Ooi's model (Ooi and Wong, 1997) to optimize the rolling piston compressor geometry using a non-dominated sorting genetic algorithm. After validating the model with respect to nine sets of working conditions for an R22 rolling piston compressor to within ±5%, they found that the optimization of 18 geometrical parameters can reduce the compressor power consumption by 10% while maintaining virtually the same compressor cooling capacity.

Ooi (2008) numerically assessed the performance of a rolling piston compressor where carbon dioxide was the working fluid. The compressor was simulated using Ooi's model (Ooi and Wong, 1997) after its validation against three experimental tests of a 32.5 cm^3 rolling piston compressor designed for R22 which demonstrated accuracy to within ±5.5%. The author concluded that, since the density of the CO_2 is higher than that of the R22, the compressor has to be scaled down and found that, due to lower leakage and frictional losses, it is more efficient to operate a compressor with lower cylinder height at higher speed than it is to operate a compressor with higher cylinder height compressor at lower speed.

Li (2012, 2013) developed and validated a semi-empirical model for reciprocating, scroll and rotary compressors. The model coupled a physical-based model for a constant speed compressor with the physical characteristics of volumetric efficiency and isentropic efficiency at different rotational speeds. Overall, the model required fifteen parameters that have to be identified starting from experimental data and using a procedure to minimize the error between experimental and model-based results. The model was able to calculate refrigerant mass flow rate, compressor electrical power and refrigerant temperature at compressor discharge given the refrigerant suction and discharge conditions. The model was validated with experimental data finding that the root mean square errors for refrigerant mass flow rate, compressor power input and discharge temperature were accurate to within ±3%, ±3% and ±3 K respectively.

Lee et al. developed (Lee et al., 2015) and validated (Lee et al., 2016) a deterministic model of a two-stage rotary compressor. The validation considered an R410A rolling piston compressor and 16 experimental test conditions. The agreement between calculated and experimental data was within –6.09% to +2.90%

for cooling capacity and within –3.17% to +3.49% for compressor electrical power.

Ba et al. (2016) analysed the gas dynamics of a rotary compressor using a three-dimensional computational fluid dynamics (CFD) model coupled with a dynamic grid technique. The simulated results were compared with experimental results from a rotary compressor working with R410A. The agreement between the numerical results of the cooling capacity and the experimental tests was within ±5.5% while the electrical power calculated for the compressor agreed to within ±4.9% of the experimentally measured power.

Finally, Liu et al. (2016) developed a deterministic model of a novel vapour injection rotary compressor. The model was validated both for a traditional rolling piston compressor without vapour injection and for a vapour injection one, finding that heating capacity and power consumption agreed to within ±3% for the former case and within ±6% and ±7% respectively for the latter.

All the papers previously discussed introduce useful models of a rolling piston compressor. However, with the sole exception of Li's model (Li, 2012, 2013), they are all deterministic, i.e. they require a detailed description of the compressor geometry as mandatory input for the model in order to compute compressor operating conditions. Deterministic models are nevertheless extremely useful whenever compressors have to be sized because, at this stage, a detailed analysis of the influence of geometrical (e.g. bearing and cylinder diameters, valve width and thickness, clearances etc.) or mechanical (e.g. vane spring stiffness) parameters on compressor performance is needed. Yet, when the goal of the compressor simulation is to calculate only macroscopic performance, namely the suction refrigerant mass flow rate and the compressor electrical power, simpler models may be effectively used. Indeed, unlike deterministic models, these simpler models can accurately compute compressor the main compressor operating parameters without detailed information about the geometry of the compressor, which is usually known solely to the manufacturer of the compressor itself only, or without providing too much information about compressor operation (e.g. velocities or forces acting on compressor components).

In the scientific literature, semi-empirical simulation tools for the simulation of reciprocating (Negrão et al., 2011; Winandy et al., 2002b), scroll (Dardenne et al., 2015; Winandy et al., 2002a) and screw (Giuffrida, 2016) compressors have been successfully introduced. These semi-empirical models are generally simpler than the deterministic models, but have nevertheless proven capable of reliably calculating the refrigerant mass flow rate and the compressor electrical power as a function of the operating conditions without a detailed description of the geometry of the compressor. Indeed, in these models, a thermodynamic equivalent path for the refrigerant from compressor suction to the compressor discharge is considered and a number of physical meaningful parameters, generally calculated starting from experimental or catalogue data, are introduced to describe all the different processes considered. Therefore, the goal of this paper is to introduce and validate a semi-empirical model of a rolling piston compressor capable of calculating the compressor's most important macroscopic parameters, namely the refrigerant mass flow at compressor suction and the compressor electrical power, as a function of the operating conditions without requiring detailed information on compressor geometry. The model developed is a semi-empirical one and it is alternative to the one proposed by Li (2013) with the additional advantage of reducing the input parameters from fifteen (Li, 2013) to eight, both for fixed speed and variable speed compressors. Ultimately, the proposed model is an accurate tool which is capable of reliably predicting the compressor macroscopic performance and which can be easily integrated into vapour compression system simulation with little information needed about its geometry.

2. Model description

The semi-empirical model of the rolling piston compressor is developed by taking inspiration from the scientific literature that deals with the simplified modelling of reciprocating, scroll and screw compressors (Dardenne et al., 2015; Giuffrida, 2016; Li, 2012, 2013; Winandy et al., 2002b), which breaks down the process that the refrigerant undergoes from compressor suction to compressor discharge into a thermodynamic equivalent path which physically represents all of the transformations experienced by the refrigerant inside the compressor. Fig. 1 shows the equivalent refrigerant path considered in the present model, which consists of the following steps:

(1) Isobaric heat transfer of the sucked mass flow rate at compressor suction (SUC → 1).
(2) Isobaric mixing of the sucked mass flow rate with the internal leakage mass flow rate (1 → 2).
(3) Isobaric mixing with the re-expansion refrigerant trapped in the clearance volume (2 → 3).
(4) Isentropic compression from the suction pressure up to the internal discharge pressure inside the isentropic compressor IC (3 → 4).
(5) Isenthalpic expansion from the internal discharge pressure to the actual discharge pressure through the discharge valve (4 → 5).
(6) Isobaric heat transfer of the discharge mass flow rate at compressor discharge (5 → DIS).

Each sub-process is described through the equations that are detailed in the following sections.

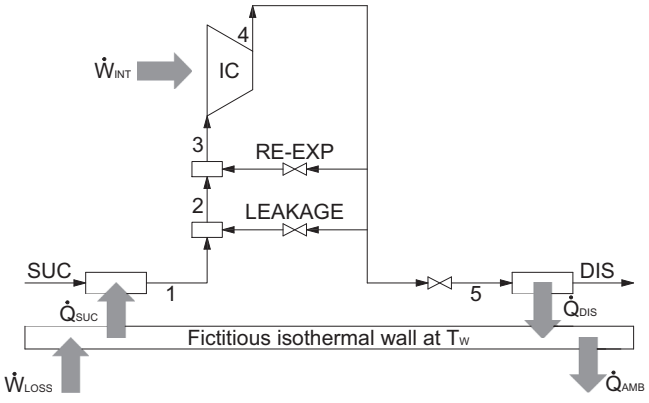

Fig. 1 – Schematic diagram of the proposed compressor model.

2.1. *Isobaric heat transfer of the sucked mass flow rate at compressor suction*

The isobaric heat transfer at the compressor suction is accounted for by introducing a fictitious isothermal wall that represents the compressor casing with a lumped parameter approach and assuming that this wall is able to account for all of the heat transfer modes inside the compressor as in previous similar studies (Dardenne et al., 2015; Giuffrida, 2016; Winandy et al., 2002a, 2002b). The following equations apply to the isobaric heat transfer process:

$$\dot{Q}_{SUC} = \dot{m}_{SUC}(h_1 - h_{SUC}) = \varepsilon_{SUC}\dot{m}_{SUC}c_{P,SUC}(T_W - T_{SUC}) \tag{1}$$

$$\varepsilon_{SUC} = 1 - e^{-NTU_{SUC}} \tag{2}$$

$$NTU_{SUC} = \frac{1}{\dot{m}_{SUC}c_{P,SUC}}(UA)_{SUC,REF}\left(\frac{\dot{m}_{SUC}}{\dot{m}_{REF}}\right)^{0.8} \tag{3}$$

Variations in the overall heat transfer coefficient with respect to the refrigerant mass flow rate are accounted for using Eq. (3) where the Reynolds heat transfer analogy is introduced and the exponent 0.8 is chosen as representative of a fully developed turbulent flow. In previous equations, $(UA)_{SUC,REF}$ stands for the reference overall heat transfer coefficient during the isobaric heat transfer process at compressor suction whereas $\dot{m}_{REF}$ stands for the reference refrigerant mass flow rate and is calculated considering the compressor swept volume as discussed in Sec. 3.1. Both are parameters of the model.

2.2. *Isobaric mixing of the sucked mass flow rate with the internal leakage mass flow rate*

In the present model, for the sake of simplicity, flank and tip leakages that arise during the compression process are modelled using a lumped parameter approach (Dardenne et al., 2015; Giuffrida, 2016). According to this approach, the leakage mass flow rate is assumed to have the same thermodynamic properties found at the isentropic compressor outlet and to take place before the suction of the same isentropic compressor as shown in Fig. 1. The leakage mass flow rate mixes with the suction mass flow rate through an isobaric mixing process that is described by the following equations:

$$\dot{m}_2 = \dot{m}_{SUC} + \dot{m}_{LEAK} \tag{4}$$

$$\dot{m}_2 h_2 = \dot{m}_{SUC}h_1 + \dot{m}_{LEAK}h_4 \tag{5}$$

where h_4 is calculated as shown in Sec. 2.4. The leakage mass flow rate is computed considering the isentropic expansion of a compressible gas through a simply convergent nozzle (Dardenne et al., 2015; Giuffrida, 2016):

$$\dot{m}_{LEAK} = \rho(p_{THR,LEAK}, s_4)A_{LEAK}\sqrt{2[h_4 - h(p_{THR,LEAK}, s_4)]} \tag{6}$$

In Eq. (6), A_{LEAK} stands for the throat area of the convergent nozzle and is a parameter of the model. The throat pressure $p_{THR,LEAK}$ is calculated assuming that the leaked refrigerant behaves like a perfect gas and, consequently, taking the maximum between the actual pressure at the nozzle outlet and the critical pressure for adapted nozzle behaviour:

$$p_{THR,LEAK} = max[p_1, p_{CRIT,LEAK}] = max\left[p_1, p_4\left(\frac{2}{\gamma_4 + 1}\right)^{\frac{\gamma_4}{\gamma_4 - 1}}\right] \tag{7}$$

2.3. *Isobaric mixing with the re-expansion refrigerant trapped in the clearance volume*

Like reciprocating compressors, rolling piston compressors are built with a discharge valve in order to avoid refrigerant back-flow from discharge to suction chamber. The volume enclosed between the discharge valve and the cylinder chamber is usually referred to as the clearance volume. The high pressure refrigerant trapped in this volume is not swept by the rolling piston but it re-expands back to the compression chamber leading to pulse back-flow and related secondary pressure pulses (Kawaguchi et al., 1986; Yanagisawa and Shimizu, 1983). In the proposed model, secondary pressure oscillations are neglected, the low pressure in the cylinder chamber is assumed to be equal to suction pressure and the refrigerant back-flow rate is modelled with reference to the isentropic flow of a compressible gas through a simply convergent nozzle, as for the leakage flow rate. This concurs with the detailed modelling proposed by Nieter et al. (1994) and leads to the following equations for the prediction of refrigerant back-flow rate:

$$\dot{m}_{RE-EXP} = \rho(p_{THR,RE-EXP}, s_4)A_{RE-EXP}\sqrt{2[h_4 - h(p_{THR,RE-EXP}, s_4)]} \tag{8}$$

$$p_{THR,RE-EXP} = max[p_1, p_{CRIT,RE-EXP}] = max\left[p_1, p_4\left(\frac{2}{\gamma_4 + 1}\right)^{\frac{\gamma_4}{\gamma_4 - 1}}\right] \tag{9}$$

Again, in Eq. (8) A_{RE-EXP} represents the throat area of the equivalent nozzle and is a parameter of the model. Since, as stated, the low pressure inside the cylinder chamber is considered equal to the suction pressure, the following equations apply:

$$\dot{m}_3 = \dot{m}_2 + \dot{m}_{RE-EXP} \tag{10}$$

$$\dot{m}_3 h_3 = \dot{m}_2 h_2 + \dot{m}_{RE-EXP}h_4 \tag{11}$$

However, an analysis of Eqs. (6)–(9) shows that in the present model the only difference between the leakage mass flow rate and the re-expansion mass flow rate is the equivalent area. Therefore, a new equivalent area, A_{TOT}, can be defined in order to reduce the number of the parameters of the model:

$$A_{TOT} = A_{LEAK} + A_{RE-EXP} \tag{12}$$

leading to

$$\dot{m}_{TOT} = \dot{m}_{LEAK} + \dot{m}_{RE-EXP} = \rho(p_{THR}, s_4)A_{TOT}\sqrt{2[h_4 - h(p_{THR}, s_4)]} \tag{13}$$

where, for the sake of clarity, as can be inferred comparing Eq. (7) and Eq. (9):

$$p_{THR} = p_{THR,LEAK} = p_{THR,RE-EXP} = max[p_1, p_{CRIT}] = max\left[p_1, p_4\left(\frac{2}{\gamma_4+1}\right)^{\frac{\gamma_4}{\gamma_4-1}}\right] \quad (14)$$

Consequently, Eqs. (4), (5), (10) and (11) become:

$$\dot{m}_3 = \dot{m}_{SUC} + \dot{m}_{TOT} \quad (15)$$

$$\dot{m}_3 h_3 = \dot{m}_{SUC} h_1 + \dot{m}_{TOT} h_4 \quad (16)$$

Finally, the following equation, where V_{IC} represents the swept volume of the isentropic compressor and is a parameter of the model, is used to calculate the refrigerant mass flow rate sucked by the isentropic compressor itself:

$$\dot{m}_3 = \rho(p_3, h_3)\dot{v}_{IC} = \rho(p_3, h_3) V_{IC} f \quad (17)$$

2.4. *Isentropic compression from the suction pressure up to the internal discharge pressure inside the isentropic compressor vc*

The compression process that the refrigerant undergoes in the compressor IC is assumed to be isentropic (Dardenne et al., 2015; Giuffrida, 2016; Li, 2012, 2013; Winandy et al., 2002a, 2002b) from the suction pressure up to the internal discharge pressure. Since, as stated, a rolling piston compressor is built with a discharge valve, the internal discharge pressure found inside the compression chamber at the end of the compression process is always greater than the actual discharge pressure. This stems from the need to overcome the discharge valve resistance and allow the refrigerant to flow through the discharge valve itself. This process is different from that found in other compressor technologies, such as the scroll and the screw compressors, which lack a discharge valve but are built with a discharge port. Indeed, in these compressors the internal discharge pressure depends on a geometrical parameter of the compressor, the built-in volume ratio, and may be lower (under-compression) or higher (over-compression) than the actual one. The actual discharge pressure is reached after a sudden refrigerant backflow from the compressor discharge plenum to the compression chamber (a state of under-compression) or a sudden refrigerant expansion (a state of over-compression) that arises as soon as the discharge port opens. In a previous study about reciprocating compressors (Winandy et al., 2002b), the discharge valve is simply modelled introducing a constant pressure drop while in the present paper this model is updated since it is considered too simplified. The internal discharge pressure is determined by considering that, in steady-state conditions, the mass flow rate at compressor suction ($\dot{m}_{SUC}$) flows entirely through the discharge valve only if the internal discharge pressure is high enough to allow for this flow. Consequently, taking the flow through the discharge valve to be an isentropic flow of a compressible gas through a simply convergent nozzle, as done for the leakage flow rate (Sec. 2.2) and for the clearance volume re-expansion (Sec. 2.3), the following equations are used to identify the internal discharge pressure:

$$\dot{m}_{SUC} = \rho(p_{THR,DIS}, s_4) A_{DIS} \sqrt{2[h_4 - h(p_{THR,DIS}, s_4)]} \quad (18)$$

$$h_4 = h(p_4, s_4) = h(p_4, s_3) \quad (19)$$

$$p_{THR,DIS} = max[p_{DIS}, p_{CRIT,DIS}] = max\left[p_{DIS}, p_4\left(\frac{2}{\gamma_4+1}\right)^{\frac{\gamma_4}{\gamma_4-1}}\right] \quad (20)$$

In Eq. (18), A_{DIS} stands for the area of the discharge valve and is a parameter of the model. Once Eqs. (18)–(20) are solved, the internal discharge pressure and the overall refrigerant state at the isentropic compressor IC discharge are calculated allowing for the calculation of the sum of leakage and re-expansion mass flow rates according to Eq. (13).

2.5. *Isenthalpic expansion from the internal discharge pressure down to the actual discharge pressure through the discharge valve*

The expansion of the refrigerant flow rate through the discharge valve is treated as an isenthalpic process from compressor internal discharge pressure down to actual discharge pressure and is described using the following equations:

$$h_5 = h_4 \quad (21)$$

$$p_5 = p_{DIS} \quad (22)$$

2.6. *Isobaric heat transfer of the discharge mass flow rate at compressor discharge*

The isobaric heat transfer at the compressor discharge is described using the same set of equations used to describe the isobaric heat transfer at the compressor suction, Eqs. (1)–(3), with some minor variations:

$$\dot{m}_{DIS} = \dot{m}_5 \quad (23)$$

$$\dot{Q}_{DIS} = \dot{m}_{DIS}(h_5 - h_{DIS}) = \varepsilon_{DIS}\dot{m}_{DIS} c_{P,5}(T_5 - T_W) \quad (24)$$

$$NTU_{DIS} = \frac{1}{\dot{m}_{DIS} c_{P,5}} (UA)_{DIS,REF} \left(\frac{\dot{m}_{DIS}}{\dot{m}_{REF}}\right)^{0.8} \quad (25)$$

In Eq. (25), $(UA)_{DIS,REF}$ stands for the reference overall heat transfer coefficient during the isobaric heat transfer process at compressor discharge and is a parameter of the model.

2.7. *Compressor electrical power input and closure equations*

In the present model, the overall compressor electrical power input is considered to be equal to the sum of two terms, namely the compressor internal power and the compressor electromechanical losses (Dardenne et al., 2015; Li, 2012, 2013; Winandy et al., 2002b):

$$\dot{W}_{COMP} = \dot{W}_{INT} + \dot{W}_{LOSS} \quad (26)$$

The first term that appears in Eq. (26) represents the compressor internal power given to the refrigerant and is calculated with the following equation:

$$\dot{W}_{INT} = \dot{m}_3 (h_4 - h_3) \tag{27}$$

On the other side, the second term that appears in Eq. (26) represents the electro-mechanical losses and is calculated according to the model proposed by Winandy et al. (2002b):

$$\dot{W}_{LOSS} = \alpha_{LOSS} \dot{W}_{INT} + \dot{W}_{LOSS,REF} \left(\frac{f}{f_{REF}} \right)^2 \tag{28}$$

In the previous equation, α_{LOSS} represents a simple, linear dependence of the electro-mechanical losses with the compressor internal power, $\dot{W}_{LOSS,REF}$ is the reference compressor electro-mechanical loss and f_{REF} is the reference compressor rotational frequency. The first two terms are parameters of the model, while the last needs to be set once as discussed in Sec. 3.1.

In the open literature, sophisticated formulations for calculating compressor to ambient thermal loss calculation are proposed (Giuffrida, 2017). The present model, by contrast, uses the following simpler formulation is used to calculate it (Giuffrida, 2016):

$$\dot{Q}_{AMB} = (UA)_{AMB} (T_W - T_{AMB})^{5/4} \tag{29}$$

where $(UA)_{AMB}$ represents the compressor-to-ambient overall heat transfer coefficient and is a parameter of the model.

Finally, the closure equation of the model is the heat balance applied to the fictitious wall in steady-state conditions:

$$\dot{W}_{LOSS} + \dot{Q}_{DIS} - \dot{Q}_{AMB} - \dot{Q}_{SUC} = 0 \tag{30}$$

Overall, eight parameters ($(UA)_{SUC,REF}$, A_{TOT}, V_{IC}, A_{DIS}, $(UA)_{DIS,REF}$, $(UA)_{AMB}$, α_{LOSS} and $\dot{W}_{LOSS,REF}$), two reference values ($\dot{m}_{REF}$ and f_{REF}) and four actual compressor working conditions (refrigerant suction pressure and temperature, refrigerant discharge pressure and shaft rotational frequency) are needed for the sucked refrigerant mass flow rate and the compressor electrical power to be calculated.

3. Results and discussion

3.1. *Compressors considered and parameters identification*

Four different hermetic rolling piston compressors manufactured by Tecumseh (2016) are used to validate the model proposed herein. These compressors are both fixed speed and variable speed compressors and have different swept volumes. They are designed for different applications (low temperature refrigeration, standard refrigeration/air conditioning and high temperature air conditioning) and operate with different refrigerants (R134a, R290 and R404A). Table 1 summarizes their main technical characteristics, while Fig. 2 provides an overview of their operating diagrams, showing that they are designed for different applications.

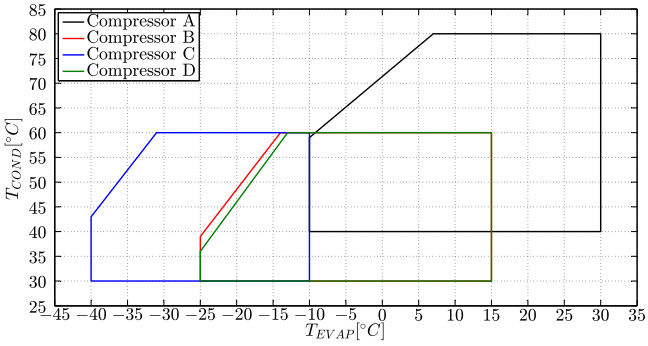

Fig. 2 – Overview of the operating diagrams of the four considered compressors.

For each compressor, the macroscopic performance, namely refrigerant mass flow rate and compressor electrical power, are taken from manufacturer selection software (Tecumseh, 2016) varying the evaporating and the condensing temperatures so as to fully cover the compressor operating diagram. For the variable speed compressor, Compressor D, the data are collected by considering three different rotational frequencies: 40 Hz, 60 Hz and 80 Hz respectively. Moreover, for each compressor, the full set of working data is split into two different subsets. The first subset, "Tuning Points", consists of the data that are used to identify the parameters of the model while the second subset, "Validation Points", contains the data used to assess the reliability of the model. Fig. 3 shows the operating diagram of each compressor together with the full set of operating conditions used to generate compressor working data and highlights the distinction between the data used to identify the parameters of the model ("Tuning points", marked by a blue diamond) and the data used to validate the ("Validation points", marked by a black circle). Moreover, Fig. 3 also shows that the "Tuning points" inside the operating diagram are not chosen in an arbitrary manner. Indeed, as discussed in Sec. 2.7, the model relies on eight parameters, which means that eight different operating conditions should be enough to identify them. However, a preliminary analysis of the number and the position of the "Tuning points" showed that, although a minimum of eight "Tuning point" is required, the model performs better if the number of the "Tuning points" is increased, but beyond a threshold value no additional improvement is found. Similarly, the performance of the model does not significantly vary

Table 1 – Main data of the four considered compressors.

Compressor	Model	Application	Refrigerant	Swept volume	Rotational frequency
A	RK5450Y UHT	High temperature air conditioning	R134a	11.4 cm^3	50 Hz
B	HGA4512U	Standard refrigeration air conditioning	R290	16.1 cm^3	50 Hz
C	RGA2426Z	Low temperature refrigeration	R404A	9.5 cm^3	50 Hz
D	THGA4445Y	Standard refrigeration air conditioning	R134a	9.5 cm^3	40 – 80 Hz

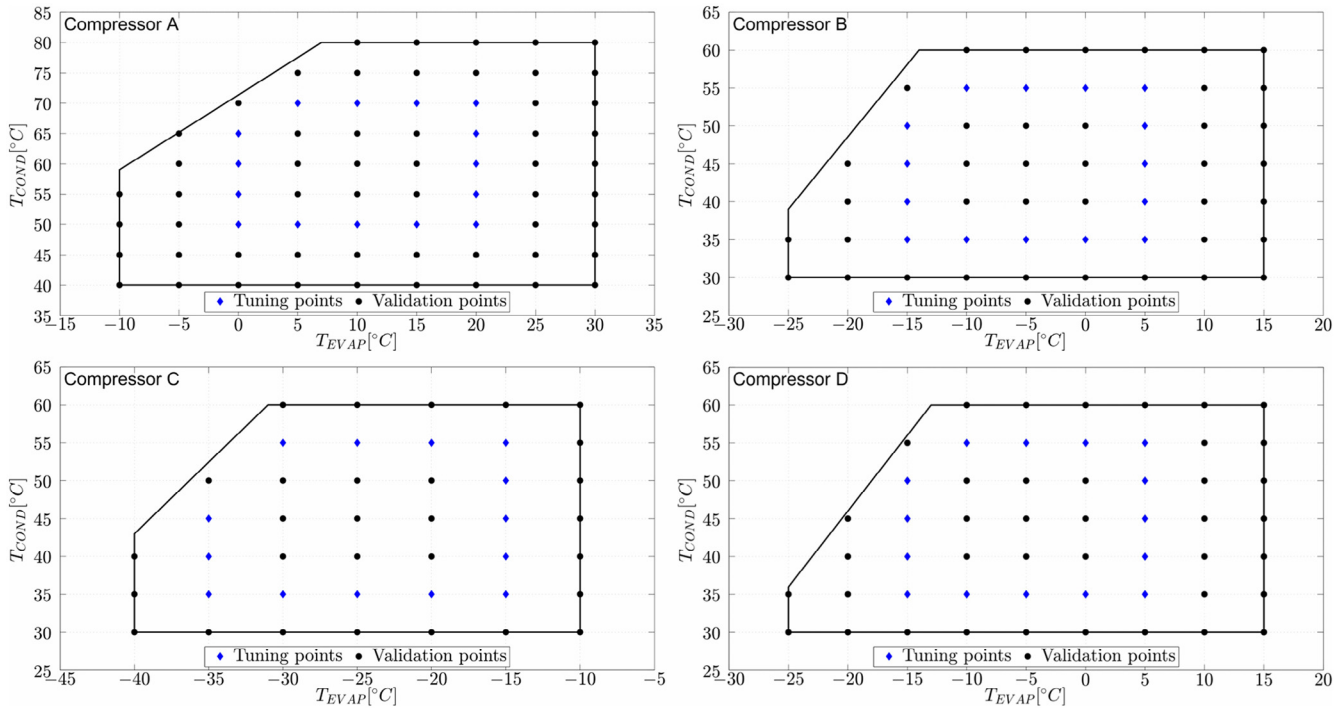

Fig. 3 – Operating diagram of each of the four considered compressors together with the tuning points and the validation points.

if the "Tuning points" are chosen close to the boundaries of the operating diagram, provided that they are evenly distributed, meaning that they have to cover both low and high evaporating and condensing temperatures. Indeed, near the boundaries of the operating diagram the sucked refrigerant mass flow rate and the compressor electrical power exhibit a large degree of variation, especially as moving from a low to a high evaporating temperature, and therefore a good choice of the "Tuning points" should consider it. As a result, the "Tuning points" are chosen at the core of the operating diagram, where the compressor is expected to typically operate for most of the time, and in order to mimic its shape for simplicity. The final choice is fifteen points for Compressors A and B, fourteen for Compressor C and forty-five (fifteen points for each of the three rotational frequencies) for Compressor D.

In order to find the eight parameters of the model ($(UA)_{SUC,REF}$, A_{TOT}, V_{IC}, A_{DIS}, $(UA)_{DIS,REF}$, $(UA)_{AMB}$, α_{LOSS} and $\dot{W}_{LOSS,REF}$), an objective function minimization procedure is considered as proposed in similar studies (Dardenne et al., 2015; Giuffrida, 2016; Li, 2012, 2013; Winandy et al., 2002b). The objective function computes the relative error between manufacturer data and calculated data according to the following equation (where n is the number of tuning points):

$$g = \sqrt{\frac{1}{2}\left[\frac{1}{n}\sum_{i=1}^{n}(e_{\dot{m},i})^2\right] + \frac{1}{2}\left[\frac{1}{n}\sum_{i=1}^{n}(e_{\dot{W},i})^2\right]} \tag{31}$$

with

$$e_{\dot{m}} = 1 - \frac{\dot{m}_{SUC,CALC}}{\dot{m}_{SUC,MAN}} \tag{32}$$

$$e_{\dot{W}} = 1 - \frac{\dot{W}_{CALC}}{\dot{W}_{MAN}} \tag{33}$$

The minimization process was carried out implementing the model described in Sec. 2 in MATLAB environment with REFPROP 9.1 (Lemmon et al., 2013) to compute the refrigerant properties and employing the multivariable function minimization routine available in the MATLAB Optimization Toolbox. Particular care was given to check that the set of parameters identified by the minimization routine leads to the global minimum of the objective function g as detailed in Sec. 3.4. Prior to the minimization procedure, the reference values of refrigerant mass flow rate (Eqs. (3) and (25)) and rotational frequency (Eq. (28)) had to be set. The choice for the calculation of the reference refrigerant mass flow rate is the multiplication of the compressor swept volume at 50 Hz by the vapour density of saturated refrigerant at 273.15 K, whereas the choice for the reference rotational frequency is the grid frequency. Therefore, the reference refrigerant mass flow rates are $\dot{m}_{REF} = 0.0082\ \mathrm{kg \cdot s^{-1}}$, $\dot{m}_{REF} = 0.0083\ \mathrm{kg \cdot s^{-1}}$, $\dot{m}_{REF} = 0.0145\ \mathrm{kg \cdot s^{-1}}$ and $\dot{m}_{REF} = 0.0069\ \mathrm{kg \cdot s^{-1}}$ for Compressor A, Compressor B, Compressor C and Compressor D respectively, whereas the reference rotational frequency is set to $f_{REF} = 50$ Hz for all the compressors. The parameters obtained at the end of the identification procedure are shown in Table 2 for the four compressors considered.

It is worth noting that the swept volume identified is generally very similar to (Compressor A, Compressor B and Compressor D) or a little higher (Compressor C) than the geometrical swept volume reported in Table 1. This result demonstrates that the proposed model together with the

Table 2 – Identified parameters of the model for the four considered compressors.

Compressor	$UA_{SUC,REF}$ [W·K^{-1}]	A_{TOT} [mm^2]	V_{IC} [cm^3]	A_{DIS} [mm^2]	$UA_{DIS,REF}$ [W·K^{-1}]	UA_{AMB} [W·K$^{-5/4}$]	$\dot{W}_{LOSS,REF}$	α_{LOSS} [–]
A	7.93	$2.49 \cdot 10^{-2}$	11.43	9.50	6.78	0.53	163	0.11
B	16.05	$9.47 \cdot 10^{-3}$	16.11	86.10	13.96	0.36	83	0.16
C	20.06	$2.44 \cdot 10^{-2}$	9.78	41.50	15.91	0.22	68	0.16
D	3.72	$5.89 \cdot 10^{-2}$	9.52	8.69	3.22	0.36	29	0.28

adopted minimization procedure correctly identifies the actual swept volume declared by the manufacturer. Moreover, the total area and discharge valve area identified seem reasonable considering the geometrical data available in Ooi and Lee (2008) and in Tan et al. (2014).

3.2. *Results for the fixed speed compressors*

The comparison between the manufacturer data for refrigerant mass flow rate and compressor electrical power and the calculated values for the three fixed speed compressors (Compressors A, B and C) is shown in Figs. 4 and 5 respectively. It is worth specifying that Figs. 4 and 5 report both the values calculated with the "Tuning Points" and those calculated with the "Validation Points" for the sake of completeness. The prediction of the refrigerant mass flow rate is highly satisfactory since, with reference to set of "Validation Points" only, overall 118 values out of 123 are predicted to within ±5% error range, while the overall error range spans –3.77% to +7.57%, with the highest or lowest values corresponding to points taken near the boundaries of the compressor operating diagram as discussed below. A similar situation can be observed regarding the prediction of the compressor electrical power, since 122 out of 123 points are calculated to within the ±5% error range, with an overall error interval of –5.78% to +3.27%; here, too, higher errors occur near the boundaries of the compressor operating diagram. Detailed results for each compressor are reported in Table 3 with respect to the number of points within the ±5% error range and to the full error range both for refrigerant mass flow rate and compressor electrical power.

A minute analysis of error distribution with respect to the operating diagram is reported in Fig. 6 for the refrigerant mass flow rate and in Fig. 7 for the compressor electrical power, both for each of the three fixed speed compressors. An analysis of these figures shows that, as previously stated, the error of the model increases as the operating condition moves from the inner area of the operating diagram towards its boundaries. Indeed, the error increases from ±3% in the central area of each operating diagram to ±5% near its boundaries, eventually exceeding 5% (absolute value) when the condensing temperature is set to the maximum allowable limit for the compressor. However, this should not be considered a weak point of the model. Indeed, as stated in the previous section, the performance of the model is found to be quite independent on the location of the "Tuning Points" inside the compressor operating diagram. Therefore, an increase in the error when operating conditions are near the boundaries of the operating diagram, i.e. when the operating conditions jeopardise safe compressor operation due to high discharge temperature (upper left corner) or electric motor overloading (upper right corner), is considered acceptable.

3.3. *Results for the variable speed compressor*

Fig. 8 shows the comparison between the manufacturer data and the calculated data of refrigerant mass flow rate (left) and compressor electrical power (right) for the variable speed compressor (Compressor D). Again, either the values calculated using "Tuning Points" and "Validation Points" are both reported for the sake of completeness. Refrigerant mass flow rate and of the compressor electrical power are both predicted satisfactorily. Indeed, with reference to the set of "Validation Points" only, 112 values out of 117 for refrigerant mass flow rate are predicted to within ±5% and 111 values out of 117 for compressor electrical power are predicted to within the same range. Overall, the error between the manufacturer data and the calculated data spans the range –5.44% to +6.86% for the refrigerant mass flow rate and –8.63% to +5.19% for the compressor electrical power. The detailed analysis of error distribution in the operating diagram is not reported since it shows the same results as the ones found for fixed speed compressors. Indeed, the error reaches its minimum or maximum value near the boundaries of the compressor operating diagram, where the operating conditions are the most dangerous for safe operation.

Table 3 – Results of the validation of the proposed model for the four compressors considering the "Validation Points" set only.

Compressor	$\dot{m}_{SUC}$		$\dot{W}_{COMP}$	
	Points within ±5%	Error range	Points within ±5%	Error range
A	53 (over 55)	–3.77% to +7.57%	55 (over 55)	–4.66% to +1.91%
B	38 (over 39)	–3.28% to +5.26%	39 (over 39)	–4.71% to +1.97%
C	27 (over 29)	–2.75% to +5.34%	28 (over 29)	–5.78% to +3.27%
D	112 (over 117)	–5.44% to +6.86%	111 (over 117)	–8.63% to +5.19%
Overall	230 (over 240)	–5.44% to +7.57%	233 (over 240)	–8.63% to +5.19%

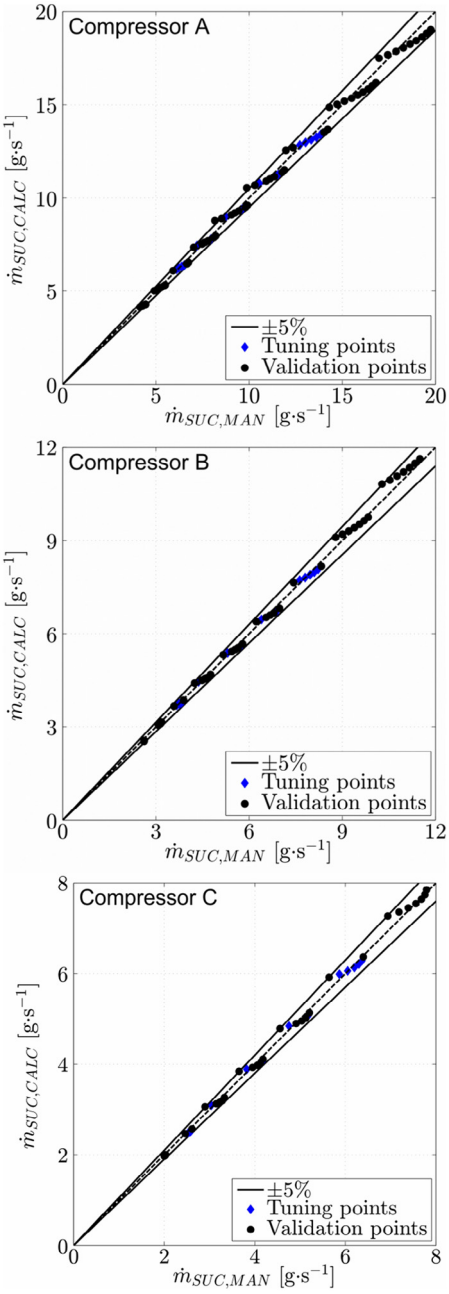

Fig. 4 – Parity plot of the suction mass flow rate for each of the three fixed speed compressors.

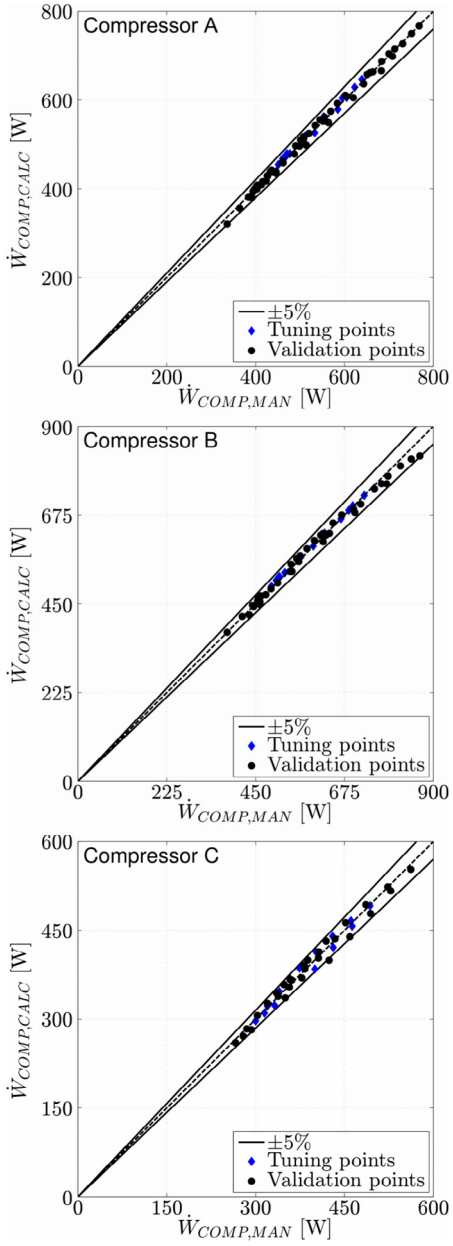

Fig. 5 – Parity plot of the compressor electrical power for each of the three fixed speed compressors.

3.4. *Sensitivity analysis*

As proposed by Cuevas et al. (2010), in order to find the most influential parameters, a sensitivity analysis of the model is carried out by considering a variation of each of the identified parameters in a ±5% range, running the model in order to calculate the relative error for each of the new set of parameters and then normalizing the result with the one found with the parameters collected in Table 2. The results of the sensitivity analysis for Compressor A are collected in Fig. 9, where it is shown that the model is highly sensitive to V_{IC} (swept volume of the isentropic compressor) and $\dot{W}_{LOSS,REF}$ (reference compressor electro-mechanical loss) whereas the remaining parameters have less influence on its performance. Moreover, it is proved that the set of parameters provided in Table 2 is the optimum one since the relative error calculated with them, i.e. with abscissa equal to 1 in Fig. 9, is the minimum one. The sensitivity analysis of the model considering the sets of parameters for Compressor B, Compressor C and Compressor D leads to the same results and, therefore, it is not reported for the sake of conciseness.

3.5. *Comparison with other non-geometrical models*

Finally, a comparison between the results achievable with the proposed model and those achievable with a simpler

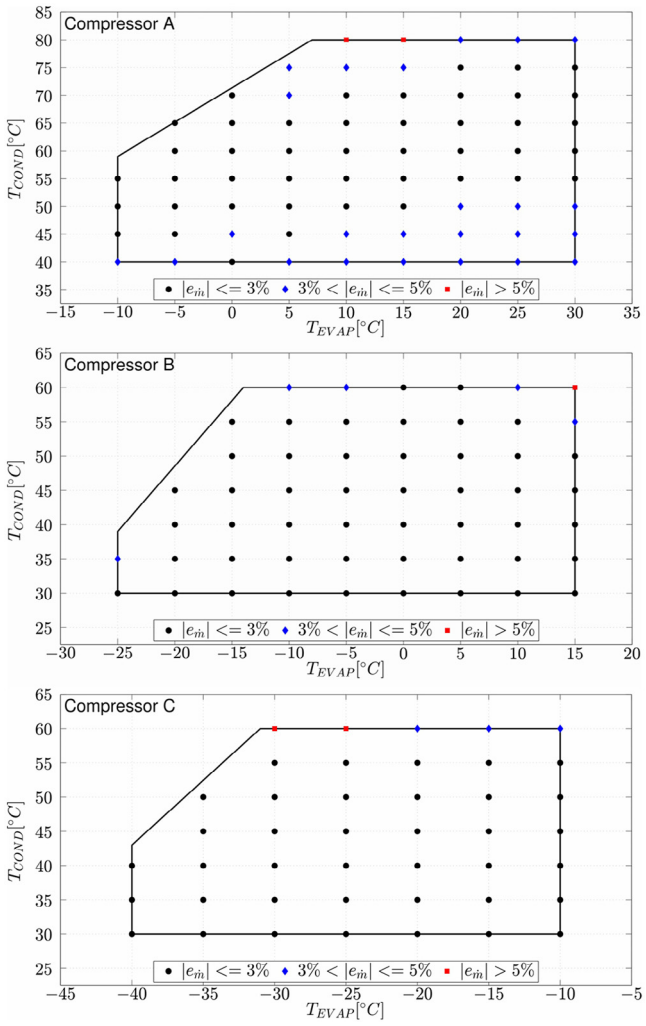

Fig. 6 – Error distribution in calculating the suction mass flow rate as a function of the position of the working point inside the compressor operating diagram.

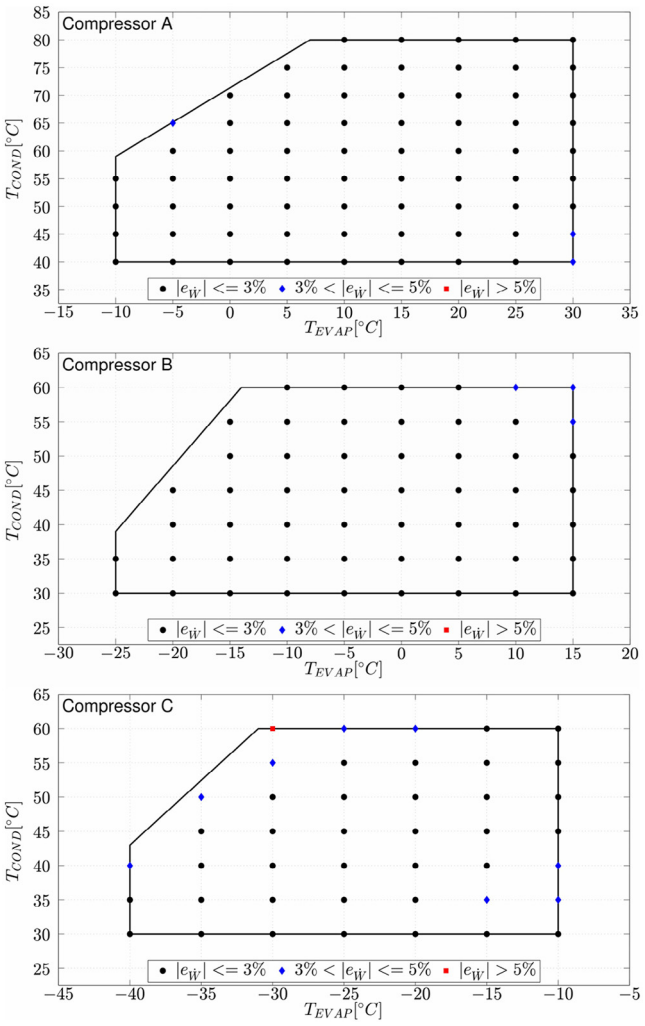

Fig. 7 – Error distribution in calculating the compressor electrical power as a function of the position of the working point inside the compressor operating diagram.

model is carried out. According to Rasmussen and Jackobsen (2000), the simplest compressor model is a black-box model which relates the compressor macroscopic performance, namely the refrigerant mass flow rate and the compressor electrical power, with the compressor operating variable, namely the evaporating and condensing temperatures. This black-box model generally takes the form of two polynomial equations like the following ones:

$$\dot{m}_{SUC} = a_0 + a_1 T_{EVAP} + a_2 T_{COND} + a_3 T_{EVAP}^2 + a_4 T_{EVAP} T_{COND} + a_5 T_{COND}^2 + a_6 T_{EVAP}^3 + a_7 T_{EVAP}^2 T_{COND} + a_8 T_{EVAP} T_{COND}^2 + a_9 T_{COND}^3 \quad (34)$$

$$\dot{W}_{COMP} = b_0 + b_1 T_{EVAP} + b_2 T_{COND} + b_3 T_{EVAP}^2 + b_4 T_{EVAP} T_{COND} + b_5 T_{COND}^2 + b_6 T_{EVAP}^3 + b_7 T_{EVAP}^2 T_{COND} + b_8 T_{EVAP} T_{COND}^2 + b_9 T_{COND}^3 \quad (35)$$

where the coefficients are found through a best fitting procedure with respect to available data. This black-box model is a simple numerical relation between the inputs and the outputs. However, although it lacks any physical significance, it is widely used by compressors manufacturers in performance specification due to its simplicity and usability, also in terms of compliance with compressors standards (EN 12900, 2013).

For the comparison purposes, the best fitting procedure is carried out for Compressor A only considering manufacturer data and using the MATLAB Curve Fitting Toolbox. The identified coefficients are reported in Table 4. Once the polynomial coefficients are known, the refrigerant mass flow rate

Table 4 – Coefficients to be used in Eqs. (34)–(35) for Compressor A.

a_0 [kg·s^{-1}]	$7.549 \cdot 10^{-3}$	b_0 [W]	$1.615 \cdot 10^{+2}$
a_1 [kg·s^{-1}·K^{-1}]	$2.694 \cdot 10^{-4}$	b_1 [W·K^{-1}]	$6.108 \cdot 10^{0}$
a_2 [kg·s^{-1}·K^{-1}]	$-2.321 \cdot 10^{-5}$	b_2 [W·K^{-1}]	$7.929 \cdot 10^{0}$
a_3 [kg·s^{-1}·K^{-2}]	$4.608 \cdot 10^{-6}$	b_3 [W·K^{-2}]	$-1.682 \cdot 10^{-1}$
a_4 [kg·s^{-1}·K^{-2}]	$6.254 \cdot 10^{-7}$	b_4 [W·K^{-2}]	$2.227 \cdot 10^{-1}$
a_5 [kg·s^{-1}·K^{-2}]	$1.978 \cdot 10^{-8}$	b_5 [W·K^{-2}]	$7.202 \cdot 10^{-2}$
a_6 [kg·s^{-1}·K^{-3}]	$3.437 \cdot 10^{-8}$	b_6 [W·K^{-3}]	$-1.194 \cdot 10^{-3}$
a_7 [kg·s^{-1}·K^{-3}]	$-5.999 \cdot 10^{-9}$	b_7 [W·K^{-3}]	$2.413 \cdot 10^{-3}$
a_8 [kg·s^{-1}·K^{-3}]	$-1.426 \cdot 10^{-8}$	b_8 [W·K^{-3}]	$-1.078 \cdot 10^{-3}$
a_9 [kg·s^{-1}·K^{-3}]	$-2.911 \cdot 10^{-9}$	b_9 [W·K^{-3}]	$5.843 \cdot 10^{-4}$

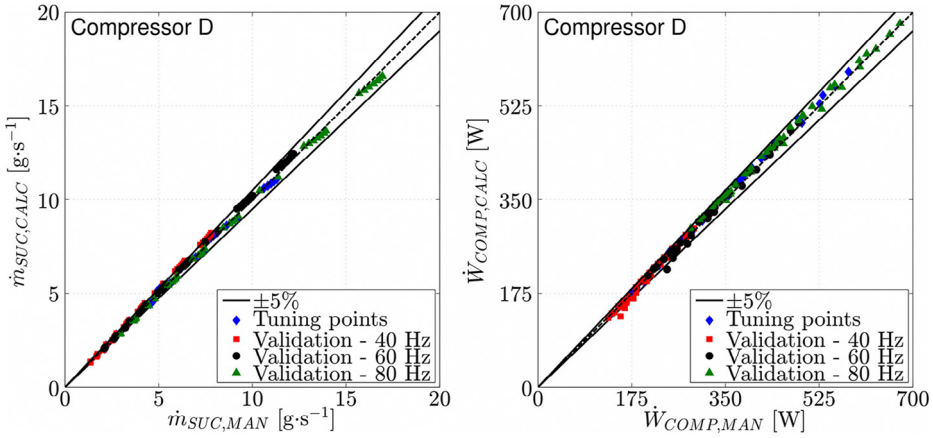

Fig. 8 – Parity plot of the suction mass flow rate (left) and parity plot of the compressor electrical power (right) for Compressor D.

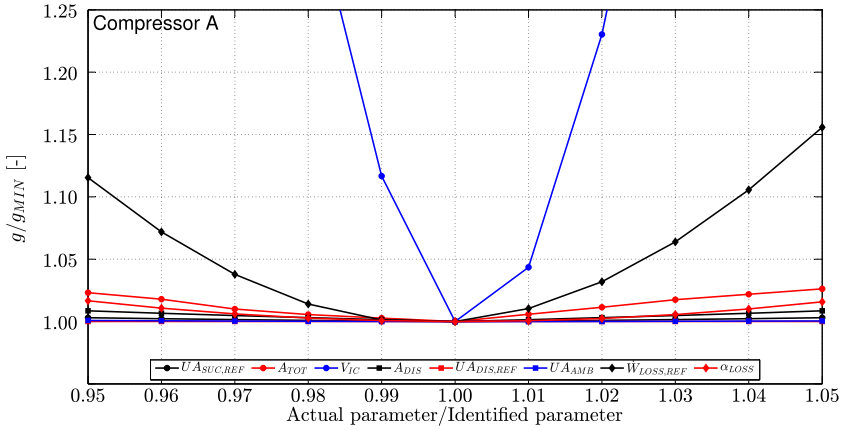

Fig. 9 – Sensitivity analysis of the compressor model to the identified parameters for Compressor A.

and the compressor electrical power are calculated and their value is compared to the manufacturer data. The ability of the black-box model to predict the refrigerant mass flow rate is strong, since all points are in the –0.67% to +0.82% range, while its ability to predict the compressor electrical power is slightly weaker since all points lie within the –4.66% to +1.91% range which, quite surprisingly, is exactly the same range found using the semi-empirical model proposed in the present paper. Consequently, it may be stated that the proposed model is slightly less accurate than the black-box model one in predicting the refrigerant mass flow rate but that it is a valid tool in predicting the compressor electrical power. However, as stated, the black-box model lacks any physical significance and, moreover, it identifies coefficients only under fixed working conditions, namely fixed suction superheating, ambient temperature and, above all, rotational frequency. As a result, if one of these parameters is varied, the polynomial coefficients are no longer valid and a new fitting procedure should be carried out leading to a new set of coefficients for the new working conditions. On the other hand, the proposed model is capable of handling variations in such parameters without any change in its coefficients and therefore it might be considered a more flexible and valuable choice of model for simulating rolling piston compressor operation.

4. Conclusions

A semi-empirical model of a rolling piston compressor is proposed in this paper. The model is a thermodynamic model, and thus does not require detailed knowledge of compressor geometry, instead requiring eight parameters to model the proposed equivalent thermodynamic process that the refrigerant undergoes from compressor suction to compressor discharge. A well-established optimization procedure that minimizes the relative error between manufacturer data and calculated data is used to identify the model parameters. The model computes refrigerant mass flow rate and compressor electrical power as a function of refrigerant suction pressure, refrigerant suction temperature, refrigerant discharge pressure and rotational frequency. The model achieves a good degree of accuracy since 96% of the calculated refrigerant mass flow rate data and 97% of the calculated compressor

electrical power data are within an error range of ±5% considering a base of 240 manufacturer data. As a result, the proposed model is a valuable tool for rotary compressor simulation and can be reliably integrated into any vapour compression system simulation tool for system design or analysis.

REFERENCES

Ba, D.-C., Deng, W.-J., Che, S.-G., Li, Y., Guo, H.-X., Li, N., et al., 2016. Gas dynamics analysis of a rotary compressor based on CFD. App. Therm. Eng. 99, 1263–1269.

Cuevas, C., Lebrun, J., Lemort, V., Winandy, E., 2010. Characterization of a scroll compressor under extended operating conditions. App. Therm. Eng. 30, 605–615.

Dardenne, L., Fraccari, E., Maggioni, A., Molinaroli, L., Proserpio, L., Winandy, E., 2015. Semi-empirical modelling of a variable speed scroll compressor with vapour injection. Int. J. Refrigeration 54, 76–87.

EN 12900, 2013. Refrigerant compressors – rating conditions, tolerances and presentation of manufacturer's performance data.

Giuffrida, A., 2016. A semi-empirical method for assessing the performance of an open-drive screw refrigeration compressor. App. Therm. Eng. 93, 813–823.

Giuffrida, A., 2017. Improving the semi-empirical modelling of a single-screw expander for small organic rankine cycles. Appl. Energy 193, 356–368.

Kawaguchi, S., Yamamoto, T., Hirahara, T., Ohinata, O., Morinushi, K., 1986. Noise reduction of rolling piston type rotary compressor. Proceedings of International Compressor Engineering Conference, 550 – 565.

Lee, S., Shim, J., Kim, K., 2015. Development of capacity modulation compressor based on a two stage rotary compressor – part I: modeling and simulation of compressor performance. Int. J. Refrigeration 54, 22–37.

Lee, S., Shim, J., Kim, K., 2016. Development of capacity modulation compressor based on a two stage rotary compressor – Part II: performance experiments and P-V analysis. Int. J. Refrigeration 61, 82–99.

Lemmon, E., Huber, M., McLinden, M., 2013. NIST standard reference database 23: Reference fluid thermodynamic and transport properties-REFPROP, version 9.1. National Institute of Standards and Technology, Standard Reference Data Program, Gaithersburg.

Li, W., 2012. Simplified steady-state modeling for hermetic compressors with focus on extrapolation. Int. J. Refrigeration 50, 1722–1733.

Li, W., 2013. Simplified steady-state modeling for variable speed compressor. App. Therm. Eng. 50, 318–326.

Liu, X., Wang, B., Shi, W., Zhang, P., 2016. A novel vapor injection structure on the blade of a rotary compressor. App. Therm. Eng. 100, 1219–1228.

Negrão, C., Erthal, R., Andrade, D., da Silva, L.W., 2011. A semi-empirical model for the unsteady-state simulation of reciprocating compressors for household refrigeration applications. App. Therm. Eng. 31, 1114–1124.

Nieter, J., Rodgers, R., Wilson A. Leyderman, F., 1994. Analysis of clearance volume equalization and secondary pressure pulse in rolling piston compressors. Proceedings of International Compressor Engineering Conference, 527 – 533.

Ooi, K., 2005. Design optimization of a rolling piston compressor for refrigerators. App. Therm. Eng. 25, 813–829.

Ooi, K., 2008. Assessment of a rotary compressor performance operating at transcritical carbon dioxide cycles. App. Therm. Eng. 28, 1160–1167.

Ooi, K., Lee, H., 2008. Multi-objective design optimization of a rotary compressor for household air-conditioning. P I Mech. Eng. E - J. Pro. 222, 241–250.

Ooi, K., Wong, T., 1997. A computer simulation of a rotary compressor for household refrigerators. App. Therm. Eng. 17, 65–78.

Rasmussen, B., Jackobsen, A., 2000. Review of compressor models and performance characterizing variables. Proceedings of International Compressor Engineering Conference, 515 – 522.

Tan, Q., Pan, S., Liu, Z., Yu, X., Feng, Q., 2014. Numerical study on transient effective flow and force areas of reed valve in a rotary compressor. P I Mech. Eng. A - J. Power Energy 228, 978–987.

Tecumseh, 2016. http://www.tecumseh.com/en/Europe/Sel_Soft_V4_0. (Accessed 5 May 2017).

Winandy, E., Saavedra O., C., Lebrun, J., 2002a. Experimental analysis and simplified modelling of a hermetic scroll refrigeration compressor. App. Therm. Eng. 22, 107–120. Winandy, E., Saavedra O., C., Lebrun, J., 2002b. Simplified modelling of an open-type reciprocating compressor. Int. J. Therm. Sci. 41, 183–192.

Yanagisawa, T., Shimizu, T., 1983. Influence of clearance volume on the performance of a rolling piston type rotary compressor. Bull. JSME 26, 537–544.